DSC determination of partial ternary phase diagrams of methanol/sodium chloride/water and propylene glycol/sodium chloride/water and their applications for synthesized diagrams

ARTICLE *in* THERMOCHIMICA ACTA · JANUARY 2011

Impact Factor: 2.18 · DOI: 10.1016/j.tca.2010.10.012

3 AUTHORS, INCLUDING:

Lindong Weng
Massachusetts General Hospital
26 PUBLICATIONS **109** CITATIONS
SEE PROFILE

Weizhong Li
Dalian University of Technology
81 PUBLICATIONS **501** CITATIONS
SEE PROFILE

Thermochimica Acta 512 (2011) 225–232

Contents lists available at ScienceDirect

Thermochimica Acta

journal homepage: www.elsevier.com/locate/tca

DSC determination of partial ternary phase diagrams of methanol/sodium chloride/water and propylene glycol/sodium chloride/water and their applications for synthesized diagrams

Lindong Weng, Weizhong Li*, Jianguo Zuo

Key Laboratory of Ocean Energy Utilization and Energy Conservation of Ministry of Education, Dalian University of Technology, Dalian, Liaoning Province 116024, PR China

ARTICLE INFO

Article history:
Received 5 August 2010
Received in revised form 11 October 2010
Accepted 21 October 2010
Available online 3 November 2010

Keywords:
Differential scanning calorimeter
Phase diagram
Synthesized ternary phase diagram
Methanol
Propylene glycol
Cryoprotectant

ABSTRACT

The present study presents partial ternary phase diagrams of methanol/sodium chloride/water and propylene glycol/sodium chloride/water systems with compositions of cryobiological interests ($R < 20$ and $x < 30$) by means of differential scanning calorimeter. To synthesize the ternary phase diagram through its relevant binary ones, the partial binary phase diagrams of methanol and propylene glycol aqueous solutions are experimentally determined as well. Ultimately, the equations characterizing the liquid surface of these two kinds of alcohol ternary systems are obtained and the polynomial representations for binary phase diagrams of methanol and propylene glycol aqueous solutions are also published in this study. The results show an excellent agreement between the experimental and synthesized data (less than ±2.5 °C) of these ternary systems. These results will enrich our understanding on the protection mechanism of these two cryoprotectants, as well as providing new evidences of the feasibility of synthesizing ternary phase diagrams of cryobiological interests.

1. Introduction

In cryobiology, phase diagrams of solutions with cryoprotectants (CPA) dissolved into a physiological salt solution are vital to better design cryopreservation protocols. On the one hand, CPA addition has become an essential step towards high post-thaw viability of cells and tissues after cryopreservation [1]. On the other hand, a phase diagram, depicting the freezing point of a certain system, can provide the basis for calculating the total equilibrium concentration of solutes and the osmotic pressure of the solution [2–4] and deepening the understanding of the protection mechanism of CPA and the reasons causing freezing injuries as well.

Therefore, both theoretical and experimental studies on phase diagrams of binary, ternary and even quaternary CPA solutions and further their osmotic behaviors have been conducted by different groups [3,5–12]. To take a CPA/sodium chloride (NaCl)/water system for instance, the typical procedure to determine the phase diagram is that the melting point T_m of the system is correlated with the total solute concentration x in g/100 g (solution) and the mass ratio of CPA over NaCl R. To be specific, the polynomial equation, a commonly used fitting model as expressed by Eq. (1), ultimately make the determination of the liquidus curve for any R value and eventually the melting point T_m corresponding to any given combination of R and x a reality [10].

$$T_m = (A + B \cdot R) \cdot x + (C + D \cdot R) \cdot x^2 + (E + F \cdot R) \cdot x^3 \quad (1)$$

where A, B, C, D, E and F are the fitting coefficients.

In particular, the recent study on glycerol/NaCl/water, Me_2SO/NaCl/water and sucrose/NaCl/water systems by Kleinhans and Mazur [2] have already demonstrated the feasibility of synthesizing the ternary phase diagram based on the corresponding binary phase diagrams. These inspiring research findings will with no doubt benefit relevant studies by allowing of determining the phase diagram of a multisolute solution with the least cost. Nevertheless, new proofs for the validity of the synthesis of the ternary phase diagram are still necessary.

Besides, thermal analysis instruments have been extensively employed to determine the phase diagrams of various systems, both organic and inorganic, such as differential thermal analysis (DTA) [13,14] and differential scanning calorimeter (DSC) [15,16]. Particularly, DSC provides a widely used and rapid method to determine, as thermometers, temperatures of phase transition, or, as calorimeters, heat capacities or enthalpies of transition in the temperature range from about 100 to 1800 K [17].

In the present study, by virtue of DSC measurement the partial ternary phase diagrams of methanol/NaCl/water and propylene glycol/NaCl/water systems are presented for the first time through generating the fitting equations for calculating the melting points

* Corresponding author. Tel.: +86 411 84708774; fax: +86 411 84708460.
E-mail address: wzhongli@dlut.edu.cn (W. Li).

0040-6031/$ – see front matter © 2010 Elsevier B.V. All rights reserved.
doi:10.1016/j.tca.2010.10.012

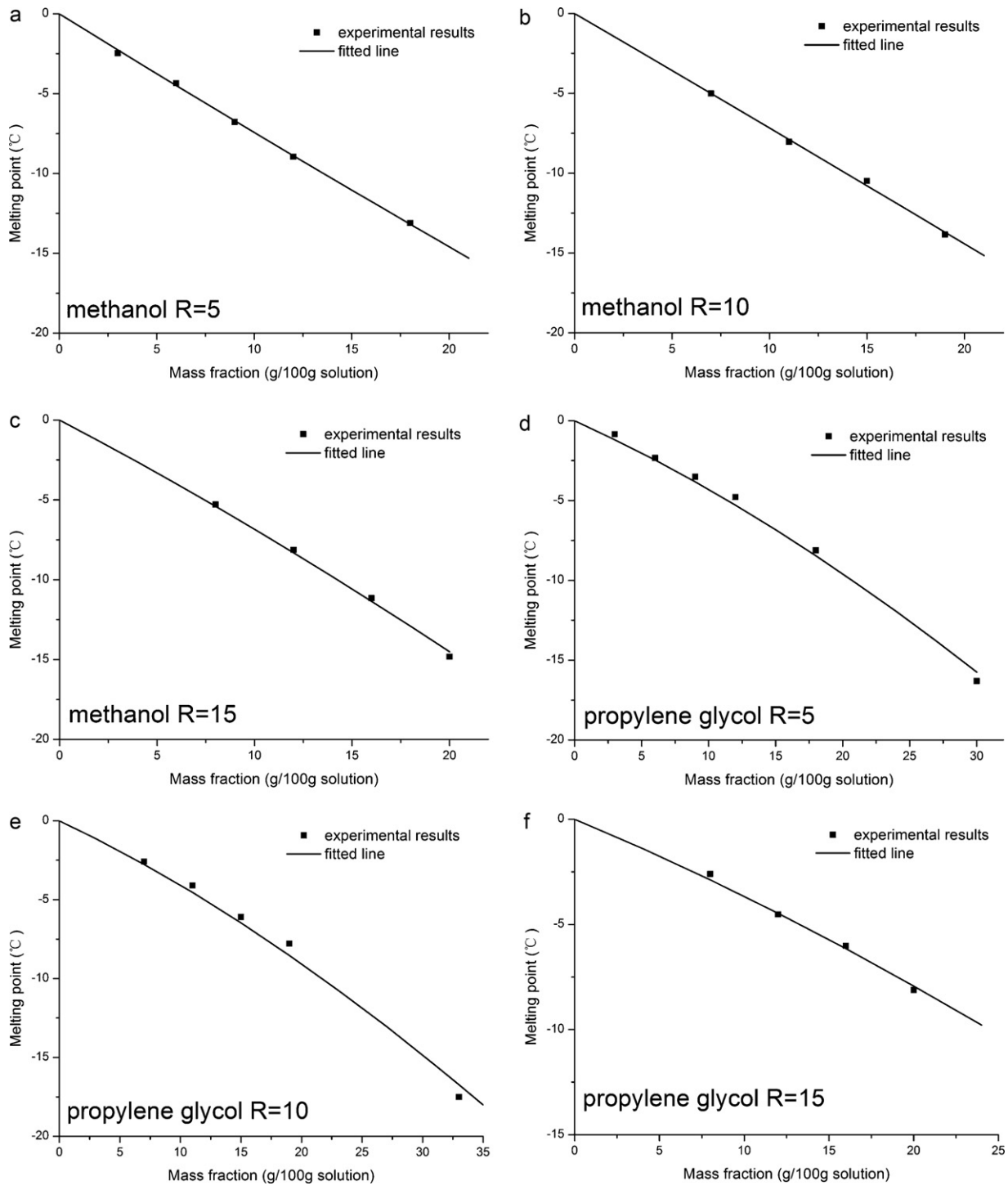

Fig. 1. Melting curves ($T_m \sim x$) for methanol/NaCl/water system of $R = 5$ (a), $R = 10$ (b) and $R = 15$ (c) and for propylene glycol/NaCl/water system of $R = 5$ (d), $R = 10$ (e) and $R = 15$ (f). (The straight lines indicate the best-fitted line according to Eq. (2) or Eq. (3); the closed squares the experimental results.)

of these two systems with compositions rich in water ($R < 20$ and $x < 30$). And the comparisons of respective actual and synthesized ternary phase diagrams of these two systems are conducted as well according to the relationships of T_m with molality m of methanol and propylene glycol aqueous solutions experimentally determined in our study and that of NaCl aqueous solution listed in Ref. [2]. What is worth mentioning is that this study concentrates on methanol and propylene glycol in respect that methanol has been demonstrated to be the least toxic additive to protect zebrafish oocytes from freezing injury [18] and propylene glycol is the most commonly used CPA in oocytes cryopreservation [19].

2. Materials and methods

2.1. Samples

Analytically pure sodium chloride (≥99.5%, mass fraction), methanol (≥99.5%, mass fraction) and propylene glycol (≥99.5%,

Table 1
Numerical data in Fig. 1(a)–(c) for the methanol/NaCl/water system.

R^b = 5			R = 10			R = 15		
Total solute mass fraction x^a (g/100 g)	Experimental result (°C)	Values given by Eq. (2) (°C)	Total solute mass fraction x (g/100 g)	Experimental result (°C)	Values given by Eq. (2) (°C)	Total solute mass fraction x (g/100 g)	Experimental result (°C)	Values given by Eq. (2) (°C)
0		0	0		0	0		0
1.5		−1.13	3		−2.14	2		−1.3
3	−2.465	−2.26	7	−5.015	−5.01	4		−2.63
4.5		−3.38	9		−6.45	6		−4
6	−4.35	−4.49	11	−8.04	−7.89	8	−5.285	−5.4
7.5		−5.59	13		−9.34	10		−6.84
9	−6.77	−6.69	15	−10.485	−10.79	12	−8.13	−8.31
10.5		−7.79	17		−12.24	14		−9.82
12	−8.95	−8.88	19	−13.845	−13.7	16	−11.15	−11.35
13.5		−9.96	21		−15.16	18		−12.91
15		−11.04				20	−14.825	−14.51
16.5		−12.11						
18	−13.1	−13.18						
19.5		−14.24						
21		−15.3						

[a] x means the total solute mass fraction of the ternary system.
[b] R means the mass ratio of CPA over sodium chloride.

Table 2
Numerical data in Fig. 1(d)–(f) for the propylene glycol/NaCl/water system.

R = 5			R = 10			R = 15		
Total solute mass fraction x (g/100 g)	Experimental result (°C)	Values given by Eq. (3) (°C)	Total solute mass fraction x (g/100 g)	Experimental result (°C)	Values given by Eq. (3) (°C)	Total solute mass fraction x (g/100 g)	Experimental result (°C)	Values given by Eq. (3) (°C)
0		0	0		0	0		0
3	−0.845	−1.19	3		−1.12	4		−1.39
6	−2.34	−2.46	7	−2.59	−2.76	8	−2.6	−2.88
9	−3.515	−3.83	11	−4.105	−4.54	12	−4.52	−4.47
12	−4.785	−5.29	15	−6.1	−6.47	16	−6.025	−6.15
15		−6.83	19	−7.785	−8.53	20	−8.115	−7.93
18	−8.115	−8.46	23		−10.72	24		−9.79
21		−10.17	27		−13.03			
24		−11.95	31		−15.47			
27		−13.81	33	−17.5	−16.73			
30	−16.305	−15.74	35		−18.01			

mass fraction) (Sinopharm Chemical Reagent Co. Ltd., Shanghai, PR China) are made into solutions using reverse osmosis and deionized water obtained from a Hitech-Kflow laboratory water purification system (Hogon Scientific Instrument Co. Ltd., Shanghai, PR China). Given that the cryobiologically interesting composition of the CPA aqueous solution, either binary or ternary, tends to be rich in water to prevent the high toxicity of the concentrated CPA solution, binary solutions of 1–5 mol/kg with an interval of 1 mol/kg and ternary solutions with $x < 30$ are prepared in our experiment to maintain the solution lowly or moderately concentrated. A maximum value of 20 for R is chosen in this study since the common compositions of CPA and NaCl in ternary systems are 1–2 M and 0.142 M respectively.

Before experimental runs, three samples are prepared for each composition for the sake of repeated measurements. Each sample (3–5 mg) is added into an aluminum sample pan sealed by the volatile sample sealer kit (Perkin-Elmer Corp., Norwalk, CT, U.S.A.) and equilibrated at 25 °C before loaded into DSC.

2.2. Differential scanning calorimeter

A Diamond DSC (Perkin-Elmer Corp., Norwalk, CT, U.S.A.) equipped with an intracooler 2P cooling accessory (providing a stable cryogenic environment as low as −85 °C) and a TAGS gas station is set up to record the thermogram of each sample during the pre-determined protocols. Prior to experiments, a two-point temperature calibration is performed using n-decane (T_m = −29.66 °C) (Sinopharm Chemical Reagent Co. Ltd., Shanghai, PR China) and reverse osmosis and deionized water (T_m = 0 °C) (Hogon Scientific Instrument Co. Ltd., Shanghai, PR China) under such scheme that the temperature range is −60 to 30 °C and the scanning rate 10 °C/min.

To obtain the melting endotherm, the samples are cooled from 25 °C to −60 °C at 50 °C/min during which the samples have nucleated completely. After held at −60 °C for 5 min to achieve an adequate equilibration, the samples are heated to the sample temperature 25 °C at a calibrated rate of 10 °C/min, meanwhile the

Table 3
The melting points of methanol/NaCl/water and propylene glycol/NaCl/water systems for x = 5 or x = 20 and R = 5 or R = 20.

	Methanol	Propylene glycol	Methanol	Propylene glycol	$T_m\|_{pg} - T_m\|_{methanol}$[a]	
	x = 5	x = 5	x = 20	x = 20	x = 5	x = 20
R = 5	−3.7609 °C	−2.0389 °C	−14.5493 °C	−9.6893 °C	1.722 °C	4.86 °C
R = 20	−3.1081 °C	−1.6246 °C	−14.4269 °C	−7.1999 °C	1.4835 °C	7.227 °C
$T_m\|_{R=20} - T_m\|_{R=5}$[b]	0.6528 °C	0.4143 °C	0.1224 °C	2.4894 °C		

[a] The subscripts indicate the values of T_m corresponding to methanol or propylene glycol solution.
[b] The subscripts indicate the values of T_m corresponding to the composition of R = 5 or R = 20.

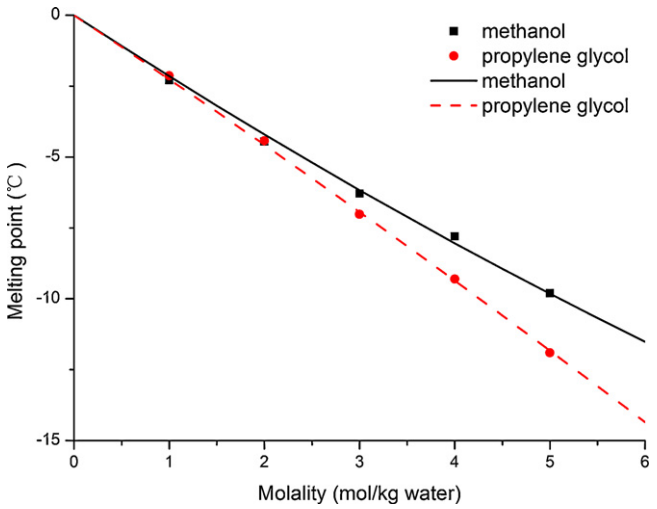

Fig. 2. Partial phase diagrams of the binary systems of methanol and propylene glycol, all in water. (The symbols represent the experimental results and lines the calculated results by Eq. (5) or Eq. (6).)

melting endotherm is recorded by the Pyris software installed in a Dell Precision T3400 workstation (Dell Inc., Round Rock, Texas, U.S.A.). Finally, the phase-transition temperature (the melting point T_m) in °C and the endothermic peak area in mJ in the thermogram are determined by means of the Pyris software.

2.3. Determination of the melting points of the binary and ternary systems

Instrumental effects, such as time or temperature lag, can affect the accuracy of DSC signals, so that several methods have been proposed to minimize such effects [20–24]. Very recently, Gosh et al. focused on and solved the instrumental effects on the melting endotherm according to which the melting point and eventually the phase diagram can be determined by DSC [24]. But, in our experiment, small doses of samples (<5 mg) are loaded into the DSC sample pans which can make the difference between the sample temperature and program temperature as minor as possible. The systems investigated in this study do not consist of any polymers and the compositions and the temperature range in our experiment cannot result in eutectics, which avoid a large time lag during the DSC detection. Hence, like what previous researchers did [10,12], the melting endotherm recorded by DSC is used directly without any further corrections.

It is important to determine the characteristic point which is able to represent the phase-transition temperature of the system investigated. In our experiment, the peak temperature T_{peak} of the melting endotherm is chosen as the phase-transition temperature rather than the onset temperature T_{onset}, the intersection point of the leading [25] or the ending edge [10] with the scanning baseline, or the revised peak temperature [12]. (In effect, the experimental data generated by the leading edge-based onset temperature has been proved to be error-prone by Woods et al.[10].) The reason why T_m is determined by T_{peak} is twofold. One of the reasons is that T_{peak} performs a good repeatability (±0.2 °C) in our experimental runs, whereas T_{onset}, based on either the leading edge or ending edge, fails to be well repeated. This is because T_{onset} is subject to the selected interval of measurement (−40 to 10 °C in our experiment), in particular in the case where the composition is far from the pure substance which will produce a scanning baseline with a relatively steep slope than a pure substance or a dilute solution does. The other is that T_{peak} for the aqueous solutions of ethylene glycol, glycerol and NaCl determined in our previous experiments well match their respective reference data given by polynomial representations in Ref. [2] (our unpublished comparisons and not presented in this study). Hence any revision as Ref. [12] did will make our experimental results deviate from the well-accepted reference data [2] unexpectedly. Despite that the direct use of T_{peak} as T_m may result in a difference as high as several degrees depending on warming rates [12], the warming rate calibrated and used in our experiment is able to minimize such difference within ±1.5 °C.

Table 4
Numerical data in Fig. 2 for methanol and propylene glycol solutions respectively.

Molality of methanol aqueous solution (mol/kg)	Experimental result (°C)	Values given by Eq. (5) (°C)	Molality of propylene glycol aqueous solution (mol/kg)	Experimental result (°C)	Values given by Eq. (6) (°C)
0		0	0		0
0.5		−1.09	0.5		−1.12
1	−2.29	−2.15	1	−2.135	−2.26
1.5		−3.19	1.5		−3.41
2	−4.455	−4.2	2	−4.425	−4.57
2.5		−5.2	2.5		−5.75
3	−6.295	−6.17	3	−7.02	−6.94
3.5		−7.11	3.5		−8.14
4	−7.795	−8.04	4	−9.305	−9.36
4.5		−8.94	4.5		−10.59
5	−9.805	−9.82	5	−11.905	−11.83
5.5		−10.68	5.5		−13.08
6		−11.51	6		−14.35

Table 5
Illustrative examples of generating synthesized ternary phase diagrams based on the corresponding binary ones.

System	Ternary system					Binary system				
	Mass ratio	Wt% NaCl + CPA (g/100 g solution)	Wt% NaCl (g/100 g solution)	Wt% CPA (g/100g solution)	Ternary melting point by Eq. (2) or (3) (°C)	NaCl molality (mol/kg)	Binary melting point by Eq. (7) (°C)	CPA molality (mol/kg)	Binary melting point by Eq. (5) or (6) (°C)	Synthesized melting point (°C)
	R	x	x_{NaCl}	x_{CPA}	MP_{ter}	m_{NaCl}	MP_{NaCl}	m_{CPA}	MP_{CPA}	MP_{syn}
Methanol/NaCl/water	5	18	3	15	−13.100	0.626	−2.105	5.709	−11.027	−13.132
Propylene glycol/NaCl/water	15	16	1	15	−6.025	0.204	−0.681	2.347	−5.386	−6.067

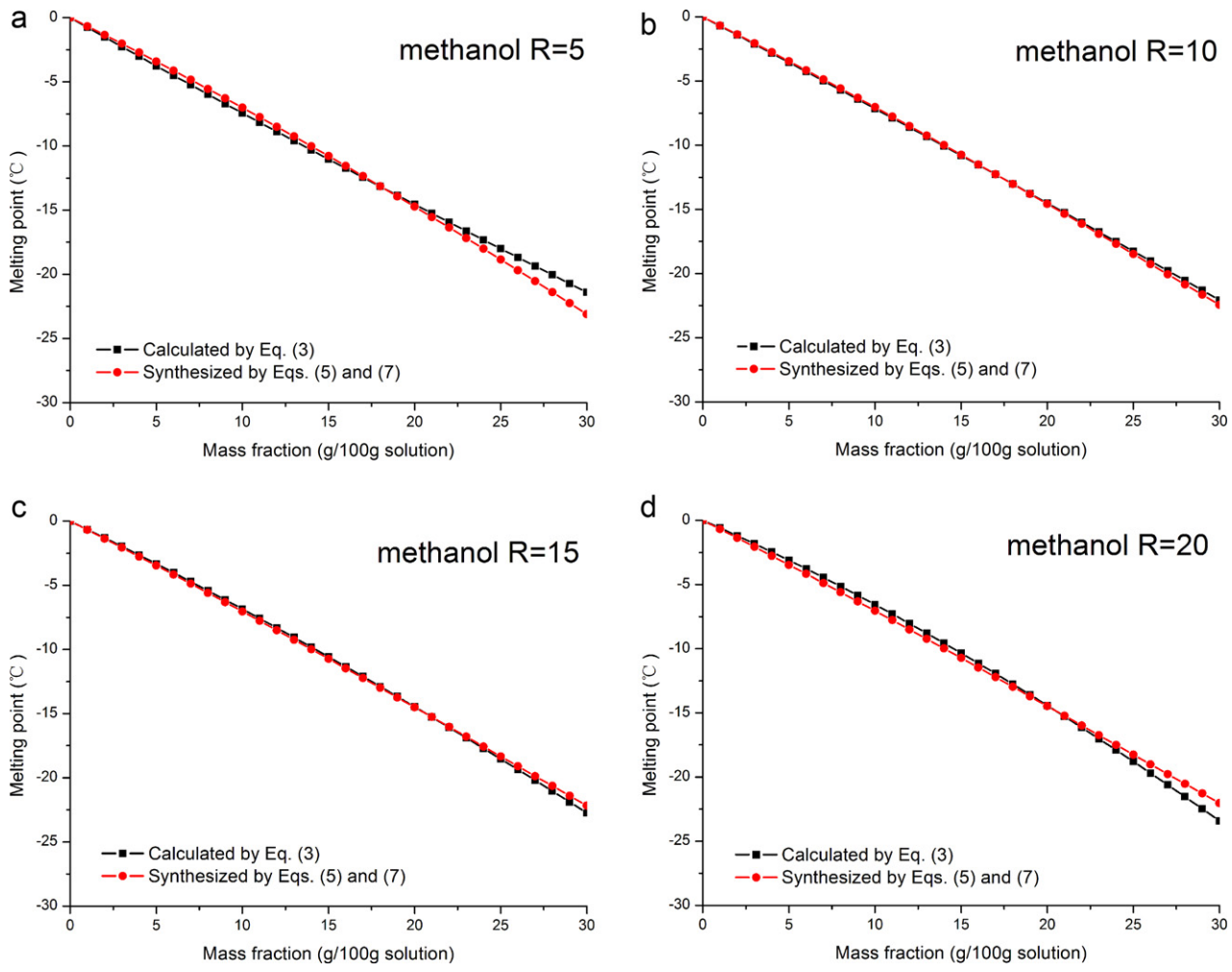

Fig. 3. Comparisons of the phase diagrams calculated by Eq. (2) for methanol/NaCl/water system of $R = 5$ (a), $R = 10$ (b), $R = 15$ (c) and $R = 20$ (d) with their corresponding synthesized ones.

3. Results and discussion

3.1. Partial ternary phase diagrams of methanol/NaCl/water and propylene glycol/NaCl/water systems

The experimentally determined melting points T_m are averaged from three measurements and correlated with the total solute concentration (mass fraction) x in g/100 g and the mass ratio R of methanol or propylene glycol over NaCl as expressed as follows:

For methanol/NaCl/water system:

$$T_m = (-0.81984 + 0.01172 \cdot R) \cdot x + (0.00493 - 0.0006156 \cdot R) \cdot x^2 + (-2.06667 \times 10^{-5} + 2.5 \times 10^{-6} R) \cdot x^3 \quad (2)$$

For propylene glycol/NaCl/water system:

$$T_m = (-0.40329 + 0.00455 \cdot R) \cdot x + (-0.00652 + 0.0001974 \cdot R) \cdot x^2 + (1.93333 \times 10^{-5} - 5 \times 10^{-7} R) \cdot x^3 \quad (3)$$

The results have been graphically displayed in Fig. 1 and the numerical values of these experimental results have been listed in Tables 1 and 2. And in this study the published values of T_m for NaCl aqueous solutions ($R = 0$) given by Ref. [2] and those for methanol and propylene glycol aqueous solutions ($R = +\infty$) determined in our study are not included in the fitting process in order to make the resulting equations predict T_m of the exact ternary phase diagrams accurately to the most extent. In effect, NaCl, dissociating into Na^+ and Cl^-, makes itself a double-effect freezing-point depressant [5,6,10] and this makes NaCl behave totally different from the case where additional components are added and, as a result, deteriorate the accuracy of a full-scale fitting. Since according to corresponding equations of $T_m \sim m$ the cubic equations for pure NaCl and pure methanol and propylene glycol aqueous solutions can be translated into $T_m \sim x$ with $R = 0$ and $R = +\infty$ respectively, the detailed expressions are not listed in the present study.

As shown in Fig. 1, more CPA added, that is a larger R, can produce a less freezing-point depression, which can also been seen in the results by others [8–10]. As a matter of fact, a larger R means more NaCl, the double-effect freezing-point depressant, are replaced by non-electrolytic CPA, which correspondingly brings about the decrease in the solutes' capability of depressing the freezing point as can be quantitatively seen in Table 3.

What can also be figured out in Table 3 is that with the same combination of R and x, T_m for propylene glycol/NaCl/water system is higher than that for methanol/NaCl/water system and this difference appears more obviously with an increasingly concentrated composition. The fact is that the existence of NaCl will make a difference in the ternary system compared with the CPA aqueous solution. From the experimental results, a conclusion can be achieved that NaCl disarranges the ternary system

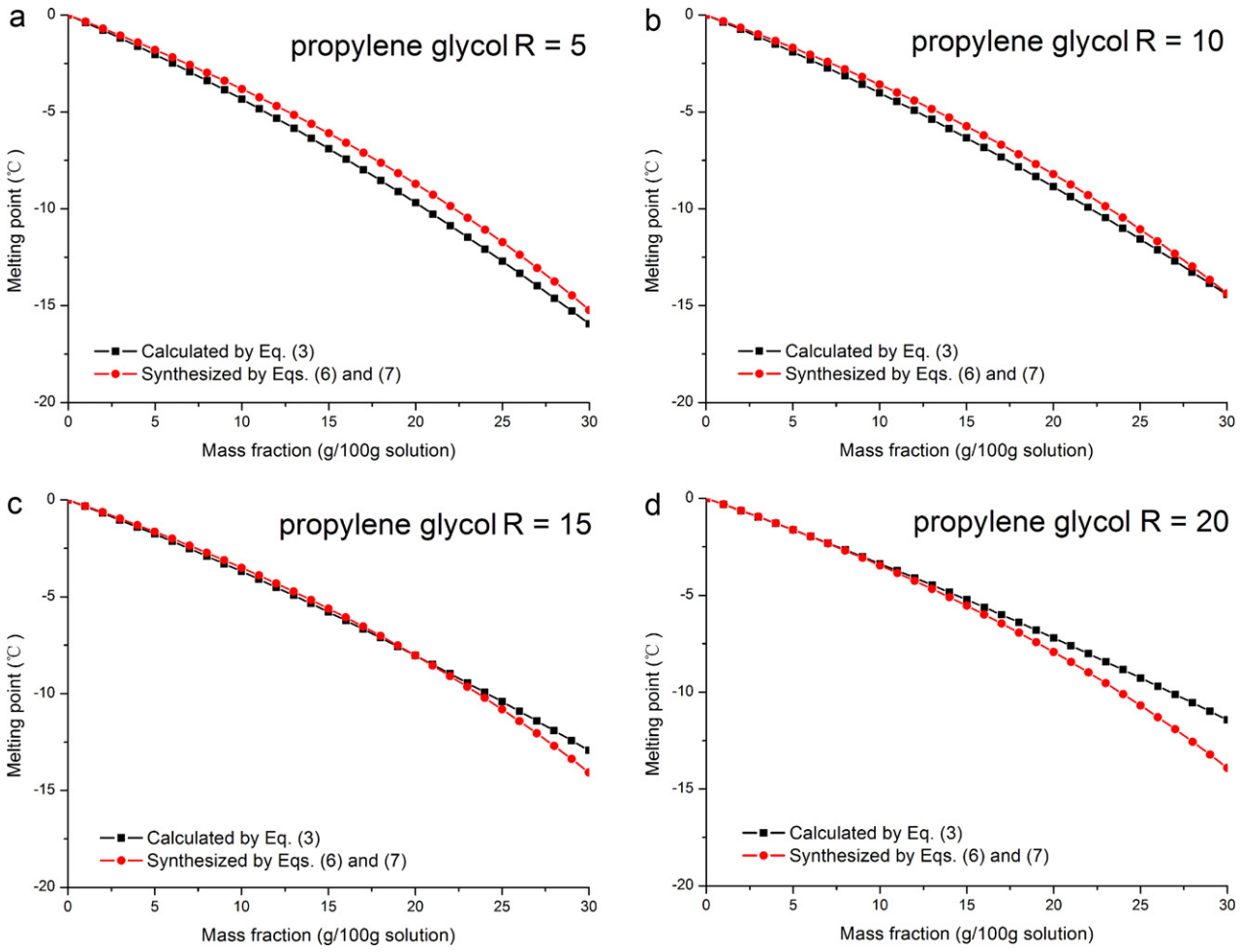

Fig. 4. Comparisons of the phase diagrams calculated by Eq. (3) for propylene glycol/NaCl/water system of $R = 5$ (a), $R = 10$ (b), $R = 15$ (c) and $R = 20$ (d) with their corresponding synthesized ones.

of propylene glycol/NaCl/water more seriously than it does for methanol/NaCl/water, which leads to the propylene glycol does not perform its original strong ability to depress the freezing-point as it does in its aqueous solutions as shown in Section 3.2. The primary reason for this phenomenon can be explained as above; however, more deep-rooted mechanisms by virtue of molecular dynamics are needed considering the role NaCl plays when added into the system.

3.2. Partial binary phase diagrams of methanol and propylene glycol aqueous solutions

To conform to the format of previous published correlations [2], a cubic equation with molality m as the independent variable is employed as follows:

$$T_m = \alpha \cdot m + \beta \cdot m^2 + \gamma \cdot m^3 \quad (4)$$

where α, β and γ are the fitting coefficients.

Ultimately, the polynomial representations for methanol and propylene glycol aqueous solutions are expressed as follows.

For methanol aqueous solution:

$$T_m = -2.1992 \cdot m + 0.0492 \cdot m^2 - 0.0004 \cdot m^3 \quad (5)$$

For propylene glycol aqueous solution:

$$T_m = -2.2992 \cdot m - 0.0285 \cdot m^2 + 0.0002 \cdot m^3 \quad (6)$$

As shown in Fig. 2 and Table 4, propylene glycol performs more actively than methanol in terms of depressing the freezing-point with the same molality, which is different from the case of ternary systems. The molecular structures of these two kinds of CPA can contribute to this phenomenon. To be specific, the molecule of propylene glycol, into which two hydroxyle groups are embedded, has approximately double capacity of hydrogen-bonding with water molecules compared with the single-hydroxyl molecule of methanol. As a result, more hydroxyle groups existing in a molecule may not only restrict more water molecules from nucleating but aggravate the depression of the freezing point by enhancing their ability to resist subcooling.

In addition, to achieve a complete foundation for synthesizing the ternary phase diagram, the polynomial representation of the binary phase diagram of NaCl aqueous solution is also listed as follows [2]:

$$T_m = -3.34 \cdot m - 0.0201 \cdot m^2 - 0.0231 \cdot m^3 \quad (7)$$

3.3. Synthesized ternary phase diagrams of methanol/NaCl/water and propylene glycol/NaCl/water systems

The synthesized ternary phase diagram is calculated according to the relevant binary phase diagrams following the procedures originally proposed by Kleinhans and Mazur [2]. In this study, two illustrative examples for methanol/NaCl/water and propylene glycol/NaCl/water systems respectively are given as seen in Table 5

Table 6
The collection of the polynomial coefficients for the ternary systems.

System	Coefficient					
	A	*B*	*C*	*D*	*E*	*F*
Methanol/NaCl/water	−0.81984	0.01172	0.00493	−0.0006156	-2.06667×10^{-5}	2.5×10^{-6}
Propylene glycol/NaCl water	−0.40329	0.00455	−0.00652	0.0001974	1.93333×10^{-5}	-5×10^{-7}

and the calculation equations are listed as follows:

$$x_{\mathrm{NaCl}} = \frac{x}{R+1} \tag{8}$$

$$x_{\mathrm{CPA}} = \frac{R \cdot x}{R+1} \tag{9}$$

$$m_{\mathrm{NaCl}} = \frac{x_{\mathrm{NaCl}}/M_{\mathrm{NaCl}}}{100 - x_{\mathrm{NaCl}} - x_{\mathrm{CPA}}} \cdot 1000 \tag{10}$$

$$m_{\mathrm{CPA}} = \frac{x_{\mathrm{CPA}}/M_{\mathrm{CPA}}}{100 - x_{\mathrm{NaCl}} - x_{\mathrm{CPA}}} \cdot 1000 \tag{11}$$

$$MP_{\mathrm{syn}} = MP_{\mathrm{NaCl}} + MP_{\mathrm{CPA}} \tag{12}$$

where x_{NaCl} and x_{CPA} are the mass fraction of NaCl and CPA respectively in g/100 g; m_{NaCl} and m_{CPA} are the molality of NaCl and CPA in mol/kg; M_{NaCl} and M_{CPA} are the molar mass of NaCl and CPA in g/mol and MP_{NaCl}, MP_{CPA} and MP_{syn} are the melting point of NaCl/water, CPA/water binary systems and the corresponding synthesized value in °C.

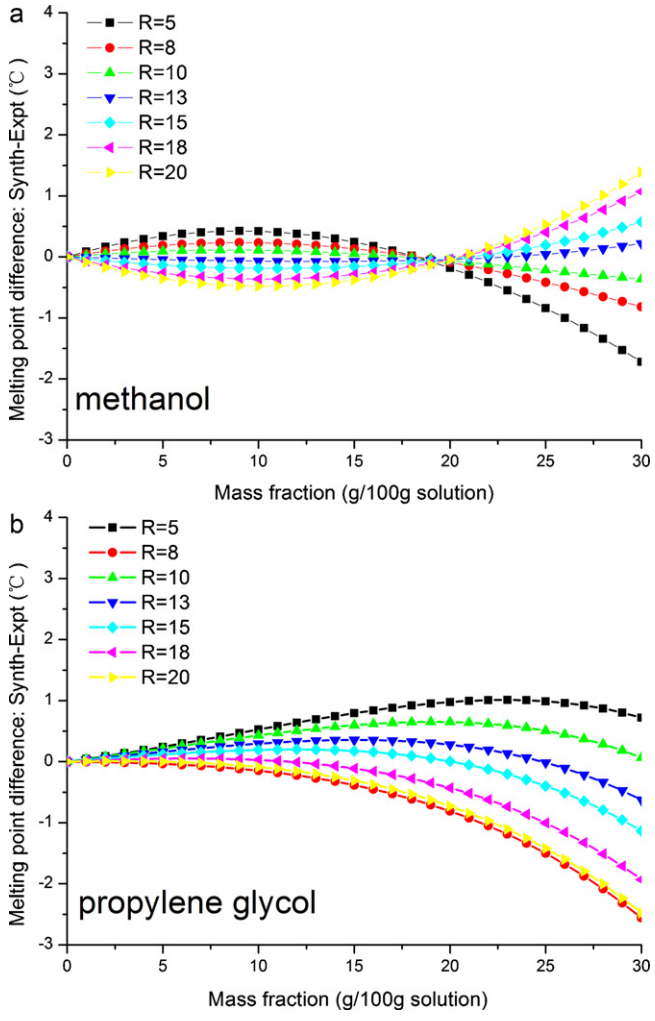

Fig. 5. The differences between the phase diagrams calculated by Eq. (2) or (3) for the ternary system methanol/NaCl/water (a) and propylene glycol/NaCl/water (b) and their corresponding synthesized ones for $R = 5$, 8, 10, 13, 15, 18 and 20.

Table 7
The collection of the polynomial coefficients for the binary systems.

System	Coefficient		
	α	β	γ
Methanol/water	−2.1992	0.0492	−0.0004
Propylene glycol/water	−2.2992	−0.0285	0.0002
NaCl/water[a]	−3.34	−0.0201	−0.0231

[a] The coefficients for the NaCl/water mixture is from Ref. [2].

The comparisons for $R = 5$, 8, 10, 13, 15, 18 and 20 have been displayed by Figs. 3 and 4. To directly investigate the differences between the results calculated by Eq. (2) or (3) and those calculated by the synthesis method, Fig. 5 is presented afterwards.

As illustrated by Figs. 3–5, the agreements between the fitting equation-derived and synthesized ternary phase diagrams are excellent (for methanol/NaCl/water less than ±1.5 °C and for propylene glycol/NaCl/water less than ±2.5 °C) in particular when it comes to the dilute cases. These findings provide other two evidences to demonstrate the feasibility of synthesizing ternary phase diagrams from corresponding binary ones.

Besides, as seen in Fig. 5, more concentrated solution will make the divergence of the synthesized ternary phase diagram from the experimental ones larger. The different physical and chemical properties of methanol and propylene glycol due to their distinct structures should give birth to totally different trends of deviation.

4. Conclusions

In the present study, the partial ternary phase diagrams of methanol/NaCl/water and propylene glycol/NaCl/water systems and the partial binary phase diagrams of methanol and propylene glycol solutions have been determined by means of DSC approach. The equations characterizing the relationships between the melting points and the compositions of these systems are presented. Furthermore, an excellent agreement between the experimental and synthesized data (less than ±2.5 °C) of the two ternary systems can be achieved. The polynomial coefficients of Eqs. (2), (3) and (5)–(7) have been collected in Tables 6 and 7. The findings in this study will be a useful supplement to the database of phase diagrams, as well as proving the feasibility of synthesizing ternary phase diagrams of cryobiological interests by two new evidences.

Acknowledgements

This research is sponsored by the National Nature Science Foundation of China (50976017) and NSFC's Key Program Projects (50736001).

Appendix A. Supplementary data

Supplementary data associated with this article can be found, in the online version, at doi:10.1016/j.tca.2010.10.012.

References

[1] B.J. Fuller, Cryoprotectants: the essential antifreezes to protect life in the frozen state, Cryo-Letters 25 (2004) 375–388.
[2] F.W. Kleinhans, P. Mazur, Comparison of actual vs. synthesized ternary phase diagrams for solutes of cryobiological interest, Cryobiology 54 (2007) 212–222.
[3] J.A.W. Elliott, R.C. Prickett, H.Y. Elmoazzen, K.R. Porter, L.E. McGann, A multisolute osmotic virial equation for solutions of interest in biology, Journal of Physical Chemistry B 111 (2007) 1775–1785.
[4] R.C. Prickett, J.A.W. Elliott, L.E. McGann, Application of the osmotic virial equation in cryobiology, Cryobiology 60 (2010) 30–42.
[5] F.H. Cocks, W.E. Brower, Phase diagram relationships in cryobiology, Cryobiology 11 (1974) 340–358.
[6] M.L. Shepard, C.S. Goldston, F.H. Cocks, The H_2O–NaCl–glycerol phase diagram and its application in cryobiology, Cryobiology 13 (1976) 9–23.
[7] G.M. Fahy, Simplified calculation of cell water content during freezing and thawing in nonideal solutions of cryoprotective agents and its possible application to the study of 'solution effects' injury, Cryobiology 18 (1981) 473–482.
[8] D.E. Pegg, Simple equations for obtaining melting points and eutectic temperatures for the ternary system glycerol/sodium chloride/water, Cryo-Letters 4 (1983) 259–268.
[9] D.E. Pegg, Equations for obtaining melting points and eutectic temperatures for the ternary system dimethyl sulphoxide/sodium chloride/water, Cryo-Letters 7 (1986) 387–394.
[10] E.J. Woods, A. Bagchi, J.D. Benson, X. Han, J.K. Critser, Melting point equations for the ternary system water/sodium chloride/ethylene glycol revisited, Cryobiology 57 (2008) 336.
[11] R.C. Prickett, J.A.W. Elliott, L.E. McGann, Application of the osmotic virial equation in cryobiology, Cryobiology (2009).
[12] X. Han, Y. Liu, J.K. Critser, Determination of the quaternary phase diagram of the water–ethylene glycol–sucrose–NaCl system and a comparison between two theoretical methods for synthetic phase diagrams, Cryobiology 61 (2010) 52–57.
[13] K. Wu, W. Cui, J. Zhang, Subsolidus binary phase diagram of $C_{12}Mn$–$C_{16}Mn$ in thermotropic phase transitions materials, Thermochimica Acta 463 (2007) 15–17.
[14] I.V. Bodnar, A.P. Bologa, B.V. Korzun, L.A. Makovetskaya, Melting temperatures of the AIBIIICVI2-type (AI–Cu, Ag; BIII–Al, Ga, In; CVI–S, Se) compounds and phase diagrams of their solid solutions, Thermochimica Acta 93 (1985) 685–688.
[15] E.Y. Shalaev, F. Franks, Equilibrium phase diagram of the water–sucrose–NaCl system, Thermochimica Acta 255 (1995) 49–61.
[16] R. Courchinoux, N.B. Chanh, Use of the "shape factors" as an empirical method to determine the actual characteristic temperatures of binary phase diagrams by differential scanning calorimetry, Thermochimica Acta 128 (1988) 45–53.
[17] E. Gmelin, S.M. Sarge, Temperature, heat and heat flow rate calibration of differential scanning calorimeters, Thermochimica Acta 347 (2000) 9–13.
[18] M. Plachinta, T. Zhang, D.M. Rawson, Studies on cryoprotectant toxicity to zebrafish (Danio rerio) oocytes, Cryo-Letters 25 (2004) 415–424.
[19] J.K. Jain, R.J. Paulson, Oocyte cryopreservation, Fertility and Sterility 86 (2006) 1037–1046.
[20] Y. Saito, K. Saito, T. Atake, Theoretical analysis of heat-flux differential scanning calorimetry based on a general model, Thermochimica Acta 99 (1986) 299–307.
[21] S.M. Sarge, Determination of characteristic temperatures with the scanning calorimeter, Thermochimica Acta 187 (1991) 323–334.
[22] A. Toda, M. Hikosaka, K. Yamada, Superheating of the melting kinetics in polymer crystals: a possible nucleation mechanism, Polymer 43 (2002) 1667–1679.
[23] R.L. Danley, New modulated DSC measurement technique, Thermochimica Acta 402 (2003) 91–98.
[24] R.C. Gosh, S. Tanaka, A. Toda, Application of a deconvolution method to construct aqueous phase diagram, Thermochimica Acta 500 (2010) 100–105.
[25] E.J. Woods, M.A.J. Zieger, D.Y. Gao, J.K. Critser, Equations for obtaining melting points for the ternary system ethylene glycol/sodium chloride/water and their application to cryopreservation, Cryobiology 38 (1999) 403–407.